

Effect of ECRH Regime on Characteristics of Short-Wave Turbulence in Plasma of the L-2M Stellarator

N.N. Skvortsova, D.K. Akulina, G.M. Batanov, G.S. Voronov, L.V. Kolik,
L.M. Kovrizhnykh, A.A. Letunov, V.P. Logvinenko, D.V. Malakhov, A.E. Petrov,
A.A. Pshenichnikov, K.A. Sarksyanyan, N.K. Kharchev

A.M. Prokhorov General Physics Institute, Russian Academy of Sciences, Moscow, RF

e-mail contact to the main author: nina@fpl.gpi.ru

Abstract The present paper reports on studies of short-wave turbulence in plasma of L-2M stellarator under markedly different conditions: with doubling the ECRH heating power (100 and 200 kW) and with restricting the plasma radius by a sector limiter. The role of such short-wave turbulence in anomalous transport can appear important for conditions of a thermonuclear reactor. Experiments were carried out in a basic magnetic configuration of the L-2M stellarator during ECRH at the second harmonic of the electron gyrofrequency (75.3 GHz) at average electron densities of $1.5\text{-}1.7 \cdot 10^{13} \text{ cm}^{-3}$. The energy lifetime was ~ 3.5 ms at $P_0 = 100$ kW and was reduced to ~ 2 ms at $P_0 = 200$ kW. When the limiter was introduced inside the plasma to a depth of 2 cm from the last closed flux surface, τ_E decreased by a factor of 1.3-1.4. Plasma density fluctuations were measured from the scattering spectra of gyrotron radiation at the second harmonic of operating frequency (~ 150 GHz). A quasioptical receiving system allowed measurements of scattered radiation from plasma regions $r/a \leq 0.6$ at scattering angles $\pi/4 \leq \theta \leq \pi/2$ ($24 \text{ cm}^{-1} \leq k_{\perp} \leq 44 \text{ cm}^{-1}$). The short-wave turbulence was studied for two radial positions of the scattering region: $r/a = 0.3\text{-}0.4$ and $r/a = 0.5\text{-}0.6$. Short-wave turbulence observed in the core plasma of the L-2M stellarator is assigned to the ETG mode instability. This type of turbulence exhibits features of strong plasma turbulence. It is experimentally established, that a change in the energy lifetime in L-2M stellarator correlates with the level of short-wave turbulence.

1. Introduction

The problem of interrelation between anomalous transport and characteristics of turbulence in toroidal magnetic confinement systems remains one of the central problems. Degradation of the energy confinement time τ_E with an increase in heating power P_0 in ECRH experiments is traced in well-known scalings: $\tau_E \propto P_0^{-0.59}$ for the ISS95 and $\tau_E \propto P_0^{-0.58}$ for LHD scaling. An even slower rise $\tau_E \propto P_0^{-0.73}$ was observed for the L-2M stellarator in the range of plasma densities $0.5\text{-}2 \cdot 10^{13} \text{ cm}^{-3}$ [1]. To explain anomalous transport, recent attention has been focused on short-wave turbulence associated with the ETG (Electron Temperature Gradient driven waves) instability (see, e.g., [2-4]). The role of such short-wave turbulence in anomalous transport can appear important for conditions of a thermonuclear reactor. Short-wave turbulence with $k_{\perp} v_{te} / \Omega_e \approx 0.2\text{-}0.4$ (where k_{\perp} is the wavenumber in the transverse direction to the magnetic field, v_{te} and Ω_e are the thermal velocity and the electron gyrofrequency) has been studied recently in tokamaks [5, 6]. In the LHD and L-2M stellarators, the excitation of short-wave turbulence with $k_{\perp} v_{te} / \Omega_e \approx 0.2$ was observed in [7, 8]. The question naturally arises of whether there are significant differences in characteristics of short-wave turbulence depending on ECRH conditions. The present paper reports on studies of short-wave turbulence in L-2M plasma under markedly different conditions: with doubling the ECRH heating power (100 and 200 kW) and with restricting the plasma radius by a sector limiter.

2. Experimental setup

Experiments were carried out in a basic magnetic configuration of the L-2M stellarator during ECRH at the second harmonic of the electron gyrofrequency (75.3 GHz) at average electron densities of $1.5\text{-}1.7 \cdot 10^{13} \text{ cm}^{-3}$. The energy lifetime was ~ 3.5 ms at $P_0 = 100$ kW and was reduced to ~ 2 ms at $P_0 = 200$ kW. When the limiter was introduced inward the plasma to a depth of 2 cm from the last closed flux surface, τ_E decreased by a factor of 1.3-1.4.

Plasma density fluctuations were measured from the scattering spectra of gyrotron radiation at the second harmonic of operating frequency (~ 150 GHz) [8,9]. The beam of the second harmonic was split by a quasioptical filter into 2 beams, one of which was passed along the plasma diameter, whereas the other was used as a reference beam at homodyne detection of scattered radiation (Fig. 1). A quasioptical receiving system allowed measurements of scattered radiation from plasma regions $r/a \leq 0.6$ at scattering angles $\pi/4 \leq \theta \leq \pi/2$ ($24 \text{ cm}^{-1} \leq k_{\perp} \leq 44 \text{ cm}^{-1}$). The short-wave turbulence was studied for two radial positions of the scattering region: $r/a=0.3\text{-}0.4$ and $r/a=0.5\text{-}0.6$ (labelled 1 and 2 in Fig. 1, respectively).

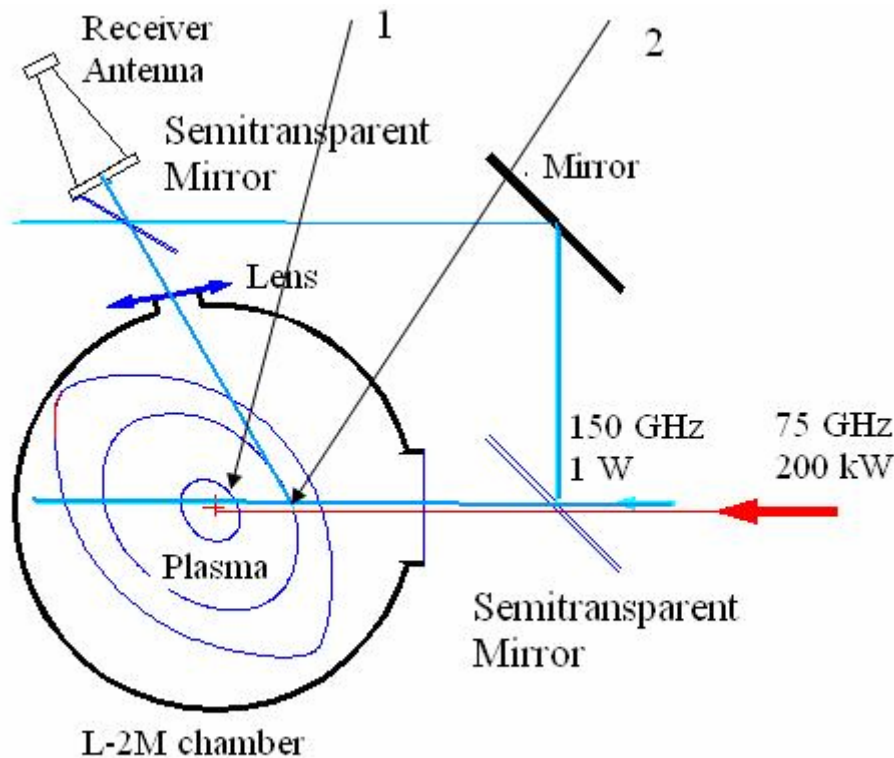


Fig. 1. Diagram of the diagnostic of collective scattering of gyrotron radiation at the second. Arrows indicate plasma regions under study.

Besides, we used small-angle scattering of ordinary waves arising due to birefringence of linearly polarized radiation of gyrotron operating frequency (75.3 GHz) in order to study long-wave density fluctuations with $k_{\perp} \approx 1 \text{ cm}^{-1}$ [10].

The upper frequency of the detector units and preamplifiers was 5 MHz. The sample rate of an analog-to-digital converter was 5 MHz.

3. Experimental results

The radial profiles of electron temperature T_e in the core region ($r/a \leq 0.6$) were measured from the intensity of electron cyclotron emission in the frequency range 69-81 GHz. At the periphery ($0.6 \leq r/a \leq 1.0$), the profiles were measured from the intensity of BIV and CIII impurity lines. The radial temperature profiles are shown in Fig. 2. The half-width of the profile is estimated as 0.4-0.5a, the maximum temperatures being $T_e = 0.65$ keV at $P_0 = 100$ kW and $T_e = 1.1$ keV at double power. A jump in the temperature was observed near the last closed flux surface, where the T_e value steeply increased by 150 eV at $P_0 = 100$ kW and by 200-250 eV at double power. The radial temperature profiles normalized to the maximal value $T_e(0)$ were similar in shape. With the limiter introduced inward the plasma, both the maximal value $T_e(0)$ and the value of temperature jump decreased; in this case, the temperature jump at the boundary was shifted inside according to the position of the limiter.

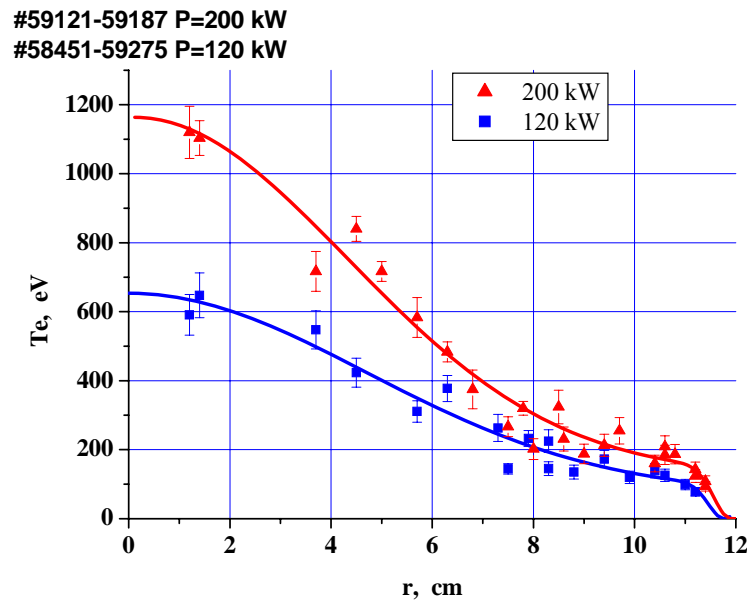


Fig. 2. Radial electron temperature profiles for two heating powers.

The radial density profiles were measured by a Michelson interferometer using a beam of an HCN laser ($337 \mu\text{m}$) over 7 chords [11]. In all the regimes, the radial profiles were typically flattened, extended from $r/a=0$ to $r/a=0.8$ and smoothly sloping at the periphery at $r/a > 0.8$. The characteristic density gradient region at $P_0 = 200$ kW approached the LCFS; in the presence of the limiter, the gradient region was shifted to $r/a \approx 0.7$. The introduction of the limiter causes the plateau part of the density profile to narrow to $r/a \leq 0.4$ at $P_0 \approx 100$ kW.

Figure 3 shows a typical time behavior of plasma characteristics (plasma density, electron temperature, plasma energy, and noise intensity measured at $r/a \sim 0.6$) in discharges without the limiter and with the introduced limiter for two values of the heating power of 100 and 200 kW.

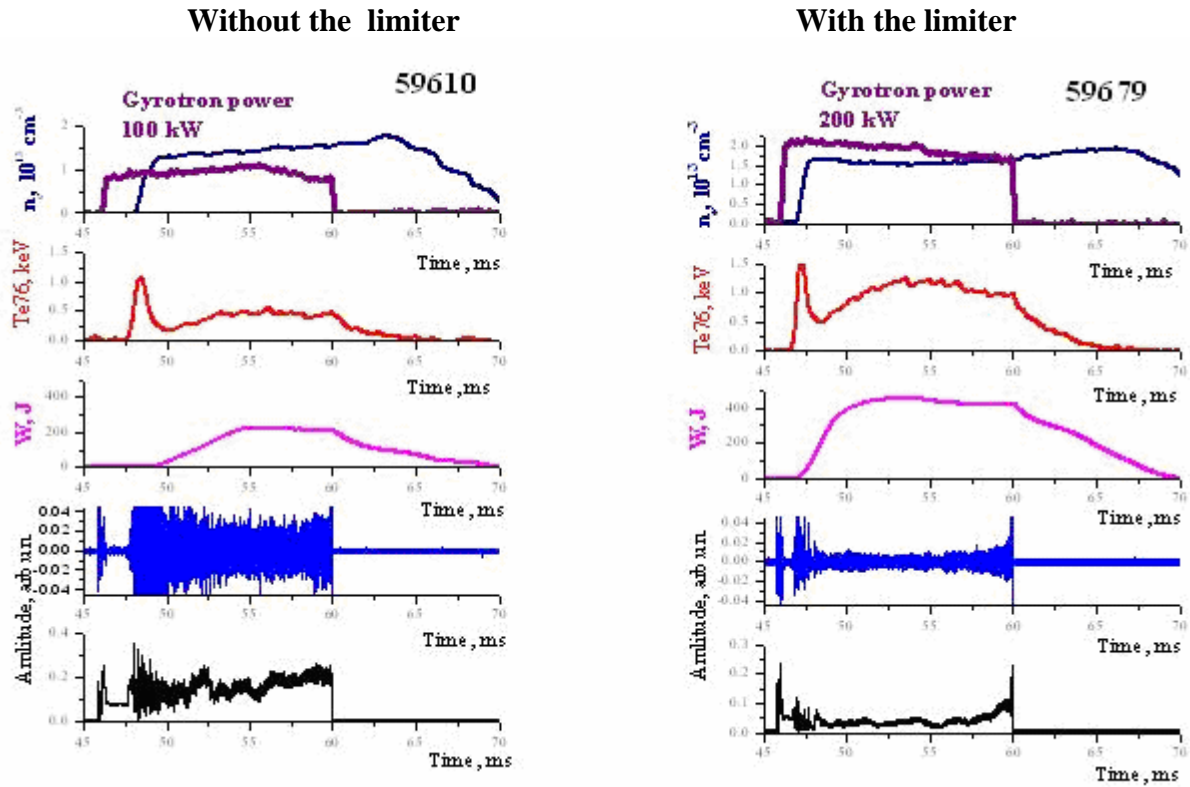


Fig. 3. Typical time behavior some plasma characteristics (from top to bottom): plasma density, gyrotron power, central electron temperature, plasma energy, and intensity of fluctuations at $r/a \sim 0.6$ with a 5 kHz filter and the intensity of the same fluctuations without the LF filter.

At $P_0 = 100$ kW and 200 kW, the Fourier spectra of scattered radiation in the frequency range 5 kHz - 1 MHz are continuous spectra with exponentially decreasing intensity and with feebly marked wide bands, which are more pronounced for the region $r/a = 0.3-0.4$ and are rather weak for $r/a = 0.5-0.6$. Accordingly, the noise spectral density for $r/a = 0.3-0.4$ is higher than that for $r/a = 0.5-0.6$ by a factor of 2-2.5.

Figure 4 shows the normalized Fourier spectra of scattered radiation at the gyrotron second harmonic averaged over 5 shots at heating power $P_0 = 100$ kW in the absence of a limiter. Solid curves are for the scattering region located 6-7 cm from the chamber axis; dashed curves for the scattering region located 4-5 cm from the chamber axis. Also shown are integrated noise densities (at frequencies above 5 kHz). On doubling the heating power to 200 kW, the Fourier spectra retain their characteristic features, but the noise density increases by one half. The limiter also provokes an increase in the spectral density at frequencies 5-50 kHz and a twofold increase in the total noise density.

When the sector limiter is introduced into the plasma, the noise spectral density increases markedly in the frequency range 5-50 kHz; as a result, the total noise density (integrated over the spectrum) increases by a factor of 1.5-2. Figure 5 shows the smoothed Fourier spectrum constructed following the Welch algorithm. The level of broadband harmonics in the presence of the limiter is reduced in this case.

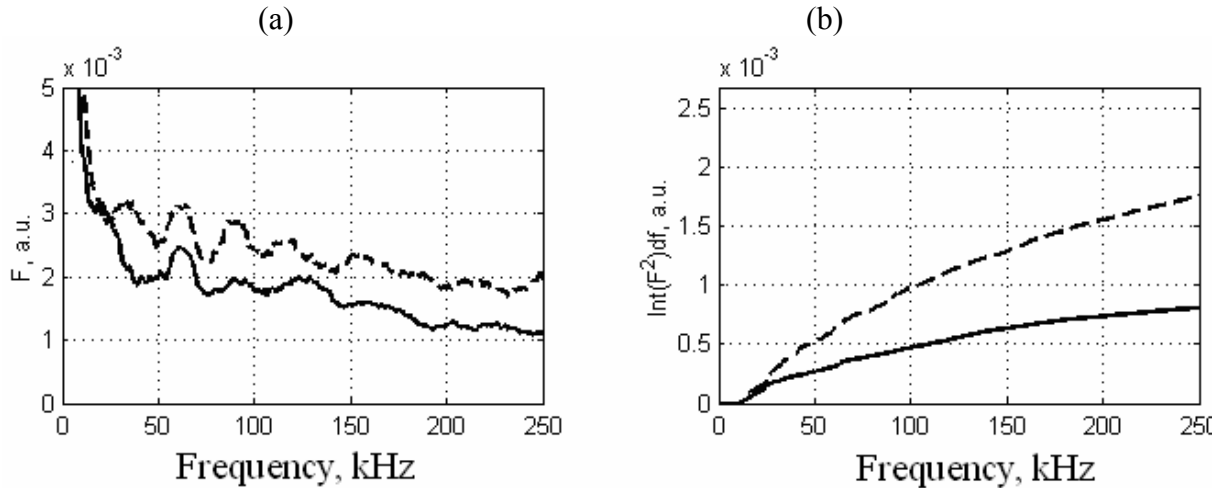


Fig. 4. (a) Fourier spectra of scattered radiation at the gyrotron second harmonic averaged over 5 shots at heating power $P_0 = 100$ kW in the absence of a limiter and (b) integrated noise densities (at frequencies above 5 kHz). Solid curves are for the scattering region located 6-7 cm from the chamber axis; dashed curves for the scattering region located 4-5 cm from the chamber axis.

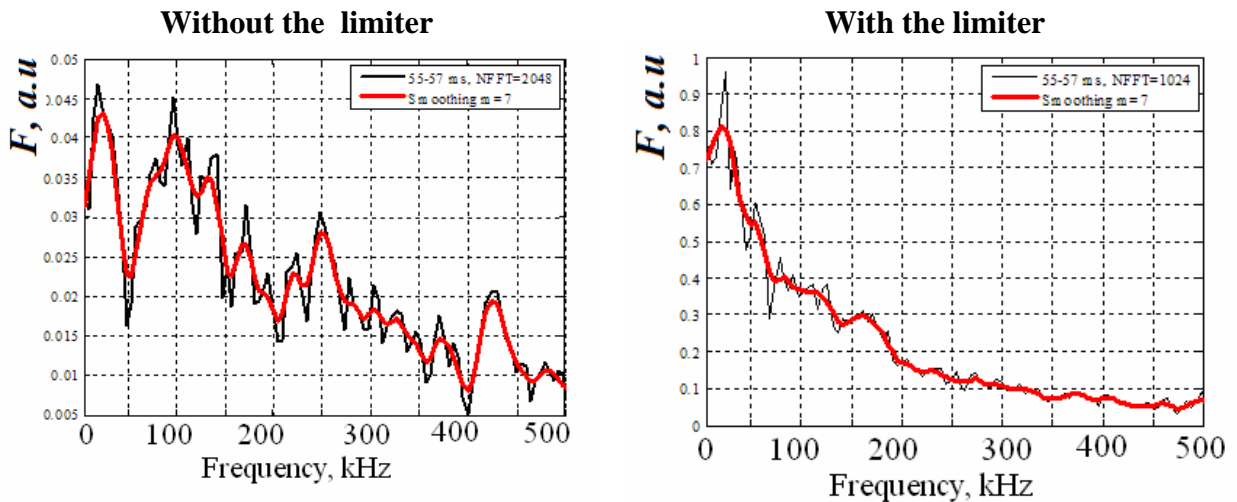


Fig. 5. Fourier spectra of small-scale fluctuations with $k=40_{\perp}$ cm $^{-1}$ at $r/a \sim 0.4$ without the limiter and with the introduced limiter. The heating power is 100 kW.

Results of measurements of long-wave turbulence (small-angle scattering of gyrotron radiation) show that the behavior of their Fourier spectra is very similar to the behavior of short-wave spectra.

Bicoherent spectra of short-wave turbulence and the crosscorrelation of short- and long-wave fluctuations were studied. The bicoherence and cross-correlation coefficients are found to be small ($\sim 1\%$). This means that, at the middle radius of the plasma column, we do not observe the transformation of the energy of the short-wave component into the long-wave fluctuations in the spectrum and do not observe a linear dependence between the excitation of short-wave and long-wave fluctuations in the same poloidal cross section.

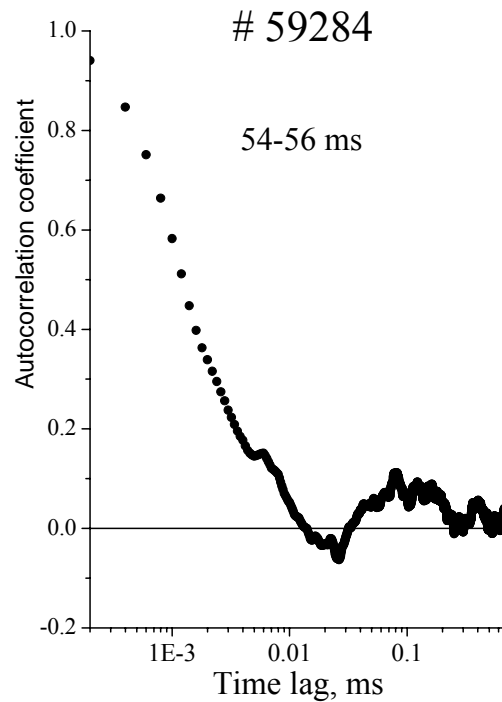


Fig. 6. Autocorrelation coefficient of small-scale fluctuations with $k=40_{\perp} \text{ cm}^{-1}$ at $r/a \sim 0.6-0.7$ in the absence of a limiter at the absence of a limiter. The heating power is 100 kW.

The autocorrelation functions (ACFs) of scattered signals measured at the middle radius and the probability density functions (PDFs) were constructed (Fig 6). The autocorrelation functions typically have extended tails with small amplitude, which imply the existence of a weak influence function ("memory"). The presence of heavy tails in comparison with Gaussian distributions (the existence of the memory in the process) as well as the presence of quasi-harmonics in the spectrum is demonstrated convincingly in the R/S analysis, operating with long time samples of fluctuations [12]. Figure 7 shows the R/S plot for fluctuations in comparison with signals corresponding to a regular and a Gaussian process, respectively. The influence of periodic components in the scattered signal is reflected in the presence of steps in the R/S signal. Thus, the analysis of probability characteristics of short-wave turbulence at the middle plasma radius allows us to identify fluctuations as the strong structural turbulence. Estimates show that these stochastic structures comprise no more than 10% of the total energy of fluctuations (for comparison, about 30 % of energy fluctuations is accumulated in stochastic plasma structures in the edge plasma of the L-2M stellarator [13]).

IV. Discussion of results and conclusion

Examining the radial electron temperature and density profiles, we can conclude that the conditions for exciting ETG instability are satisfied, and moreover, the instability threshold is far exceeded in the experiments under discussion. Measurements from the plasma regions located at different distances from the chamber axis show that most energy of noise is observed in the region with a higher electron temperature. Again, the increase in the ECR heating power is accompanied by the growth in the energy of short-wave turbulence. Numerical simulation of heat transport for condition of our experiment was performed using the model [14] assuming that the anomalous transport coefficient is proportional to T_e . With such a dependence of the anomalous transport coefficient, the calculations are in satisfactory

agreement with the experimental data, as follows from Fig. 8 which compares the results of calculations of neoclassical and anomalous heat fluxes for two values of the ECR heating power 100 and 200 kW.

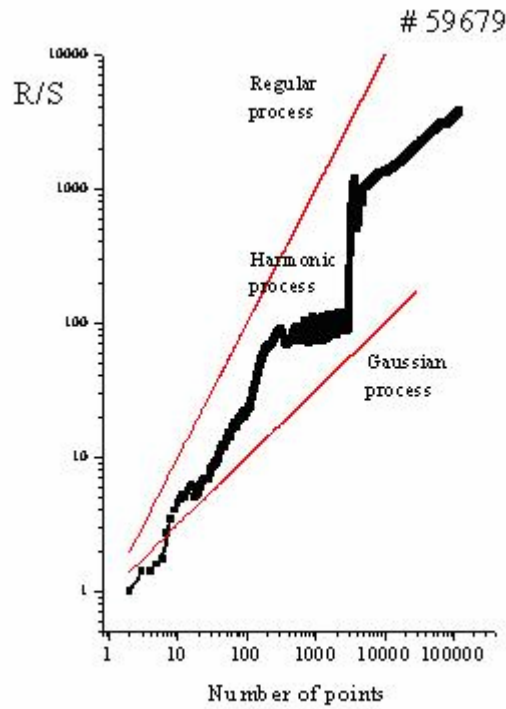


Fig. 7. R/S analysis of time samples of small-scale fluctuations with $k=40_{\perp} \text{ cm}^{-1}$ at $r/a \sim 0.6-0.7$ at a heating power of 100 kW in the absence of a limiter.

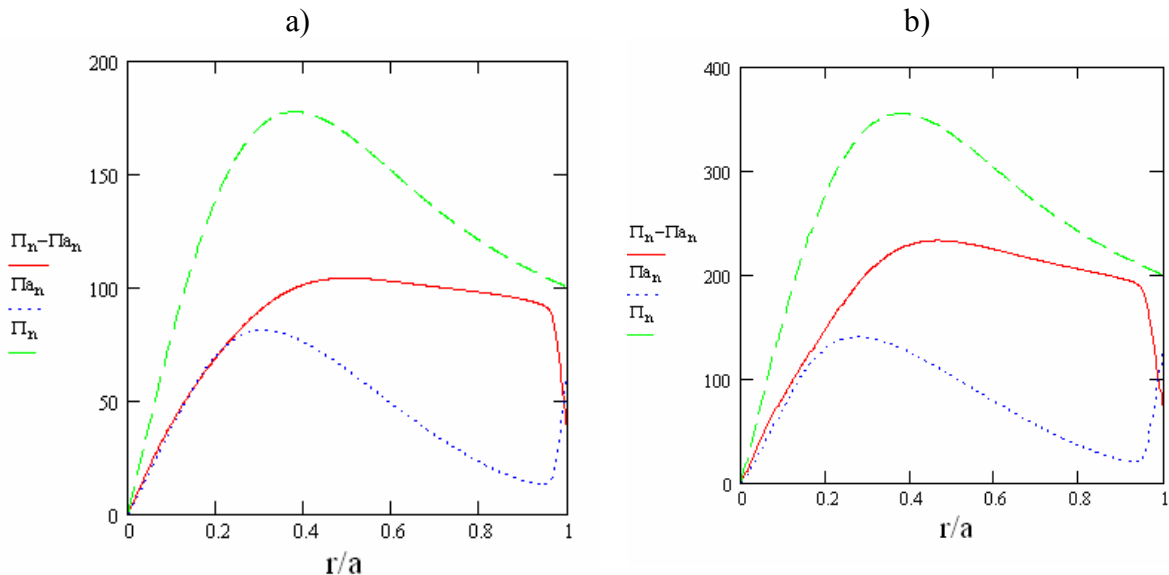


Fig. 8. Total (dashed), neoclassical (solid), and anomalous (dotted line) fluxes as functions of the normalized radius r/a for heating powers of (a) 100 and (b) 200 kW.

In summary,

1. Short-wave turbulence connected with the ETG mode instability in the core plasma of the L-2M stellarator was investigated by the method of collective scattering of gyrotron radiation at the second harmonic of operating frequency.
2. It is shown that this type of turbulence exhibits features of strong plasma turbulence.
3. It is shown that the decrease in the energy lifetime on doubling the ECR heating power correlates with the growth in the energy of short-wave turbulence, which is also confirmed by numerical calculations.
4. It is established that the cooling of the plasma near last closed flux surface by the sector limiter causes the decrease in the energy lifetime and also the growth of short-wave turbulence in the core plasma.

Thus, it is experimentally established that the energy lifetime in L-2M stellarator is correlated to the level of short-wave turbulence.

This work was supported by the RF Presidential Program of Support of Leading Scientific Schools (grant NSh-452.2008.2) and the Russian Foundation for Basic Research (project no. 06-02-16272)

REFERENCES

- [1] O.I. Fedianin, D.K. Akulina, G.M. Batanov et al. Plasma Physics Reports. 2007. **33** 280.
- [2] F. Jenko, W. Dorland, G.W. Hammet Phys. Plasmas. 2001. **8**. 4096
- [3] Li J., Kishimoto Y. Phys. Plasmas. 2004. **11**. 1493.
- [4] C.M. Ronch et al. Plasma Phys. Control. Fusion. 2005. **47**. B323.
- [5] A.D. Gurchenko, E.Z. Gusakov., A.B. Altukhov. et al. Nucl. Fusion. **47**. 245.
- [6] T.L. Rhodes, W.A. Peebles, et al. Plasma Phys. Control Fusion 2007 **49** B183
- [7] G.M. Batanov, L.V. Kolik, A.E. Petrov et al. Plasma Physics Reports. 2003. **29**. 380.
- [8] G.M. Batanov, L.V. Kolik, M.I. Petelin et al. Plasma Physics Reports. 2003. **29**. 1019.
- [9] N.N. Skvortsova, G. Batanov et al. The 35th IEEE International Conference on Plasma Science. Karlsruhe, Germany, June 15-19, 2008, 5E3
- [10] D.K. Akulina, G.M. Batanov, et al. Plasma Physics Reports. 2000. **26**. 3.
- [11] V. A. Knyasev, A.A. Letunov, V.P. Logvinenko. Instruments and Experimental Techniques. 2004. **47**.230
- [12] N. N. Skvortsova, G.M. Batanov, et al. Low-frequency structural plasma turbulence in stellarators. V. Yu. Korolev and N.N. Skvortsova. (Eds) "Stochastic Models of Structural Plasma Turbulence". VSP, Leiden - Boston, The Netherlands. 2006. 63.
- [13] G.M. Batanov, V.E. Bening, V.Yu. Korolev et al. JETP Lettrs. 73. 143
- [14] L.M. Kovrizhnykh. Plasma Physics Reports. 2006. **32**. 988.